3-D Target Localization in Wireless Sensor Networks Using RSS and AoA Measurements

Slavisa Tomic, Marko Beko, and Rui Dinis, *Senior Member, IEEE*

***Abstract*—This paper addresses target localization problems in both noncooperative and cooperative 3-D wireless sensor networks (WSNs), for both cases of known and unknown sensor transmit power, i.e., P_T. We employ a hybrid system that fuses distance and angle measurements, extracted from the received signal strength and angle-of-arrival information, respectively. Based on range and angle measurement models, we derive a novel nonconvex estimator based on the least squares criterion. The derived nonconvex estimator tightly approximates the maximum-likelihood estimator for small noise. We then show that the developed estimator can be transformed into a generalized trust region subproblem framework, by following the squared range approach, for noncooperative WSNs. For cooperative WSNs, we show that the estimator can be transformed into a convex problem by applying appropriate semidefinite programming relaxation techniques. Moreover, we show that the generalization of the proposed estimators for known P_T is straightforward to the case where P_T is not known. Our simulation results show that the new estimators have excellent performance and are robust to not knowing P_T. The new estimators for noncooperative localization significantly outperform the existing estimators, and our estimators for cooperative localization show exceptional performance in all considered settings.**

***Index Terms*—Angle-of-arrival (AoA), generalized trust region subproblem (GTRS), received signal strength (RSS), semidefinite programming (SDP), wireless localization, wireless sensor network (WSN).**

Manuscript received July 17, 2015; revised December 6, 2015 and April 8, 2016; accepted July 6, 2016. Date of publication July 11, 2016; date of current version April 14, 2017. This work supported in part by Fundação para a Ciência e a Tecnologia under Projects PEst-OE/EEI/UI0066/2014 (UNINOVA) and UID/EEA/50008/2013 (Instituto de Telecomunicações), project PTDC/EEI-TEL/6308/2014-HAMLeT, Program Investigador FCT (IF/00325/2015), as well as the grants SFRH/BPD/108232/2015, SFRH/BD/91126/2012, and Ciência 2008 Post-Doctoral Research grant. The review of this paper was coordinated by Dr. Y. Gao.

S. Tomic is with the Laboratory of Robotics and Systems in Engineering and Science (LARSyS), Instituto Superior Técnico, Institute for Systems and Robotics (ISR/IST), 1049-001 Lisboa, Portugal (e-mail: stomic@isr.ist.utl.pt).

M. Beko is with Universidade Lusófona de Humanidades e Tecnologias, 1749-024 Lisboa, Portugal, and also with the Centre of Technology and Systems (CTS), Instituto Desenvolvimento De Novas Tecnologias (UNINOVA), 2829-516 Caparica, Portugal (e-mail: beko.marko@ulusofona.pt; mbeko@uninova.pt).

R. Dinis is with Instituto de Telecomunicações, 1049-001 Lisboa, Portugal, and also with the Departamento de Engenharia Electrotécnica, Faculdade de Ciências e Tecnologia (FCT), 2829-516 Caparica, Portugal (e-mail: rdinis@fct.unl.pt).

Color versions of one or more of the figures in this paper are available online at http://ieeexplore.ieee.org.

Digital Object Identifier 10.1109/TVT.2016.2589923

I. Introduction

Wireless sensor networks (WSNs) generally refer to a wireless communication network that is composed of a number of devices, which are called sensors, allocated over a monitored region to measure some local quantity of interest [1]. Due to their autonomy in terms of human interaction and low device costs, WSNs find application in various areas such as event detection (fires, floods, and hailstorms) [2], monitoring (industrial, agricultural, health care, and environmental) [3], [4], energy-efficient routing [5], exploration (deep water, underground, and outer space) [6], and surveillance [7], to name a few. In many practical applications, data gathered by sensors are only relevant if they are associated with accurate sensors' locations; hence, the estimation of sensors' locations is a key requirement for a majority of practical applications [1].

Sensors are small, low-cost, and low-power nodes commonly deployed in a large number over a region of interest with limited to nonexisting control of their location in space, e.g., thrown out of an aeroplane for sensing in hostile environments [8]. Installing a global positioning system (GPS) receiver in each sensor would severely augment the network costs and restrict its applicability [9]. To maintain low implementation costs, only a small fraction of sensors are equipped with GPS receivers (called anchors), whereas the remaining sensors (called targets) determine their locations by using a kind of localization scheme that takes advantage of the known anchor locations [10]. Since the sensors have minimal processing capabilities, the key requirement is to develop localization algorithms that are fast, scalable, and abstemious in their computational and communication requirements.

Wireless localization schemes typically rely on range (distance) measurements [11], [12]. Depending on the available hardware, range measurements can be extracted from the different characteristics of radio signal, such as time of arrival (ToA) [13], time difference of arrival [14], round-trip time [15], angle of arrival (AoA) [16], or received signal strength (RSS) [17]–[21]. Recently, hybrid systems that fuse two measurements of the radio signal have been investigated [22]–[30]. Hybrid systems profit by exploiting the benefits of combined measurements, i.e., more available information. On the other hand, the price to pay for using such systems is the increased complexity of network devices, which increases the network implementation costs [1], [9].

The approaches in [17]–[21] and [31] consider the noncooperative and cooperative target localization problem, but the estimators are founded on RSS and distance measurements only.

The approaches in [22]–[24] are based on the fusion of RSS and ToA measurements. A hybrid system that merges range and angle measurements was investigated in [25]. Yu in [25] proposed two estimators for solving the noncooperative target localization problem in a 3-D scenario: linear least squares (LS) and optimization based. The LS estimator is a relatively simple and well-known estimator, whereas the optimization-based estimator was solved by the Davidson–Fletcher–Powell algorithm [32]. In [26], Wang *et al.* derived an LS and a maximum likelihood (ML) estimator for a hybrid scheme that combines RSS difference (RSSD) and AoA measurements. Nonlinear constrained optimization was used to estimate the target's location from multiple RSS and AoA measurements. Both LS and ML estimators in [26] are λ-dependent, where λ is a nonnegative weight assigned to regulate the contribution from RSS and AoA measurements. A selective weighted LS (WLS) estimator for the RSS/AoA localization problem was proposed in [28]. Gazzah *et al.* determined the target location by exploiting weighted ranges from the two *nearest* anchor measurements, which were combined with the serving base station AoA measurement. In [26]–[28], the authors investigated the noncooperative hybrid RSS/AoA localization problem for a 2-D scenario only. A WLS estimator for a 3-D RSSD/AoA noncooperative localization problem when the transmit power is unknown was presented in [29]. However, Chan *et al.* in [29] only investigated a small-scale WSN, with extremely low noise power. An estimator based on the semidefinite programming (SDP) relaxation technique for the cooperative target localization problem was proposed in [30]. Biswas *et al.* in [30] extended their previous SDP algorithm for pure range information into a hybrid one by adding angle information for triplets of points. However, due to the consideration of triplets of points, the computational complexity of the SDP approach increases rather substantially with the network size.

In this paper, we investigate the target localization problem in both noncooperative and cooperative 3-D WSNs. In the case of noncooperative WSNs, we assume that all targets exclusively communicate with anchors and that a single target is located at a time. In the case of cooperative WSNs, we assume that all targets communicate with any sensor within their communication range (whether it is an anchor or a target) and that all targets are simultaneously located. For both cases, a hybrid system that fuses distance and angle measurements, extracted from RSS and AoA information, respectively, is employed. By using the RSS propagation model and simple geometry, we derive a novel objective function based on the LS criterion. For the case of noncooperative WSNs, based on the squared range (SR) approach, we show that the derived nonconvex objective function can be transformed into a generalized trust region subproblem (GTRS) framework, which can be solved exactly by a bisection procedure [28]. For the case of cooperative localization, we show that the derived objective function can be transformed into a convex function by applying the SDP relaxation technique. Finally, we show that the generalization of the proposed estimators to the case where, alongside the targets' locations, the transmit power, i.e., P_T, is also unknown is straightforward for both noncooperative and cooperative localization.

Thus, the main contribution of our work is threefold. First, by using RSS and AoA measurement models, we derive a novel nonconvex objective function based on the LS criterion, which tightly approximates the ML criterion for small noise. In the case of noncooperative localization, we propose two novel estimators that significantly reduce the estimation error, compared with the state of the art. Finally, in the case of cooperative localization, we present the first hybrid RSS/AoA estimators for target localization in a 3-D cooperative WSN.

Throughout this paper, uppercase bold type, lowercase bold type, and regular type are used for matrices, vectors, and scalars, respectively. $\mathbb{R}^n$ denotes the n-dimensional real Euclidean space. The operators $\otimes$ and $(\bullet)^T$ denote the Kronecker product and transpose, respectively. The normal (Gaussian) distribution with mean μ and variance σ^2 is denoted by $\mathcal{N}(\mu, \sigma^2)$. $\mathrm{diag}(\boldsymbol{x})$ denotes a square diagonal matrix in which the elements of vector $\boldsymbol{x}$ form the main diagonal of the matrix, and the elements outside the main diagonal are zero. The N-dimensional identity matrix is denoted by $\boldsymbol{I}_N$ and the $M \times N$ matrix of all zeros by $\boldsymbol{0}_{M\times N}$ (if no ambiguity can occur, subscripts are omitted). $\|\boldsymbol{x}\|$ denotes the vector norm defined by $\|\boldsymbol{x}\| = \sqrt{\boldsymbol{x}^T\boldsymbol{x}}$, where $\boldsymbol{x} \in \mathbb{R}^n$ is a column vector. For Hermitian matrices $\boldsymbol{A}$ and $\boldsymbol{B}$, $\boldsymbol{A} \succeq \boldsymbol{B}$ means that $\boldsymbol{A} - \boldsymbol{B}$ is positive semidefinite.

The remainder of this work is organized as follows. In Section II, the RSS and AoA measurement models are introduced, and the target localization problem is formulated. Section III presents the development of the proposed estimators in the case of noncooperative localization for both known and unknown P_T values. In Section IV, we describe the derivation of the proposed estimators in the case of cooperative localization for both known and unknown P_T values. In Sections V and VI, complexity and performance analyses are presented, respectively, together with the relevant results to compare the performance of the newly presented estimators to the state of the art. Finally, Section VII summarizes the main conclusions.

II. Problem Formulation

We consider a WSN with N anchors and M targets, where the known locations of anchors are denoted, respectively, by $\boldsymbol{a}_1, \boldsymbol{a}_2, \ldots, \boldsymbol{a}_N$, and the unknown locations of targets are denoted by $\boldsymbol{x}_1, \boldsymbol{x}_2, \ldots, \boldsymbol{x}_M$ ($\boldsymbol{x}_i, \boldsymbol{a}_j \in \mathbb{R}^3$, $i = 1, \ldots, M$ and $j = 1, \ldots, N$). For ease of expression, let us define a vector $\boldsymbol{x} = [\boldsymbol{x}_1^T, \boldsymbol{x}_2^T, \ldots, \boldsymbol{x}_M^T]^T$ ($\boldsymbol{x} \in \mathbb{R}^{3M\times 1}$) as the vector of all unknown target locations, such that $\boldsymbol{x}_i = \boldsymbol{E}_i^T\boldsymbol{x}$, where $\boldsymbol{E}_i = \boldsymbol{e}_i \otimes \boldsymbol{I}_3$, and $\boldsymbol{e}_i$ is the ith column of the identity matrix I_M. We determine these locations by using a hybrid system that fuses range and angle measurements. Combining two measurements of the radio signal provides more information to the user, and it is likely to enhance the estimation accuracy, as shown in Fig. 1.

Fig. 1 shows how (a) a range-based, (b) an angle-based, and (c) a hybrid (range and angle) system operates for the case where $M = 1$ and $N = 4$. In range-based localization, each range measurement, i.e., $\hat{d}_i$, defines a circle as a possible location of the unknown target. Thus, a set of range measurements, i.e., $\{\hat{d}_1, \hat{d}_2, \ldots, \hat{d}_N\}$, defines multiple circles, and the area determined by their intersection accommodates the target [see Fig. 1(a)]. Similarly, with angle-based localization,

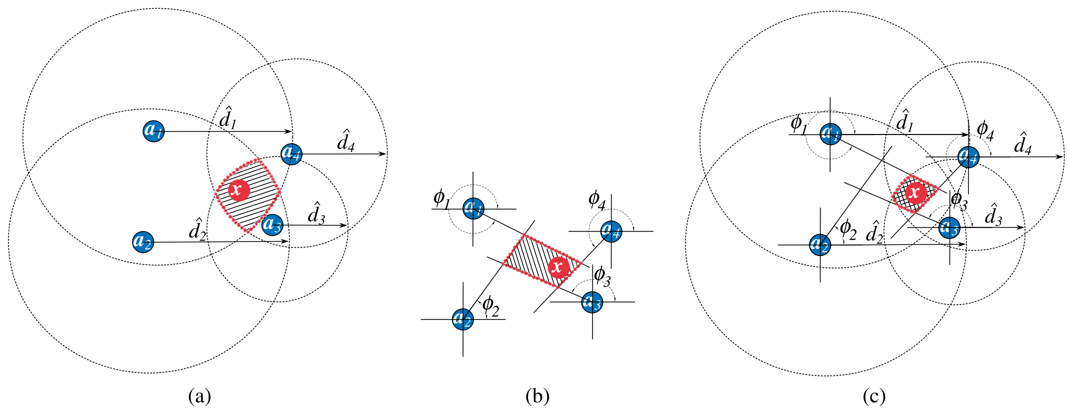

Fig. 1. Illustration of different localization systems in 2-D space. (a) Range-based localization. (b) Angle-based localization. (c) Hybrid localization.

each angle measurement, i.e., ϕ_i, defines a line as the set of possible locations of the unknown target [see Fig. 1(b)]. In Fig. 1(c), one can see that when the two measurements of the radio signal are integrated, the set of all possible solutions (the area determined by the intersection) is significantly reduced; hence, hybrid systems are more likely to improve the estimation accuracy.

Throughout this work, it is assumed that the range measurements are obtained from the RSS information exclusively, since ranging based on RSS requires the lowest implementation costs [1]. However, the RSS measurement model can be replaced with the path-loss model by using the relationship $L_{ij} = 10\log_{10}(P_T/P_{ij})$ (dB), where L_{ij} and P_{ij} are, respectively, the path loss and received power between two sensors i and j, which are within the communication range of each other (from the transmitting sensor), and P_T is the transmission power of a sensor [35], [36]. Thus

$$L_{ij}^{\mathcal{A}} = L_0 + 10\gamma\log_{10}\frac{\|\boldsymbol{x}_i - \boldsymbol{a}_j\|}{d_0} + n_{ij}, \text{ for } (i,j)\in\mathcal{A} \quad (1a)$$

$$L_{ik}^{\mathcal{B}} = L_0 + 10\gamma\log_{10}\frac{\|\boldsymbol{x}_i - \boldsymbol{x}_k\|}{d_0} + n_{ik}, \text{ for } (i,k)\in\mathcal{B} \quad (1b)$$

where L_0 denotes the path-loss value at a short reference distance d_0 ($\|\boldsymbol{x}_i - \boldsymbol{a}_j\| \geq d_0$, $\|\boldsymbol{x}_i - \boldsymbol{x}_k\| \geq d_0$); γ is the path-loss exponent (PLE) between two sensors, which indicates the rate at which the path loss increases with distance; and n_{ij} and n_{ik} are the lognormal shadowing terms modeled as $n_{ij} \sim \mathcal{N}(0, \sigma_{n_{ik}}^2)$ and $n_{ik} \sim \mathcal{N}(0, \sigma_{n_{ik}}^2)$. Furthermore, the sets $\mathcal{A} = \{(i,j) : \|\boldsymbol{x}_i - \boldsymbol{a}_j\| \leq R, \text{for } i = 1,\ldots,M,\ j = 1,\ldots,N\}$ and $\mathcal{B} = \{(i,k) : \|\boldsymbol{x}_i - \boldsymbol{x}_k\| \leq R, \text{for } i,k = 1,\ldots,M, i \neq k\}$, where R is the communication range of a sensor, denote the existence of target/anchor and target/target connections, respectively.

To obtain the AoA measurements (both azimuth and elevation angles), we assume that either multiple antennas or a directional antenna is implemented at anchors [25], [34]. To make use of the AoA measurements from different sensors, the orientation information is required, which can be obtained by implementing a digital compass at each sensor [25], [34]. However, a digital compass introduces an error in the AoA measurements due to its static accuracy. For the sake of simplicity and without loss of generality, we model the angle measurement error and the orientation error as one random variable in the rest of this paper.

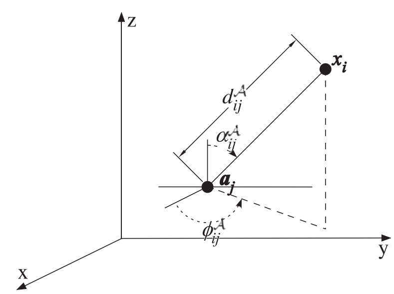

Fig. 2. Illustration of a target and anchor locations in 3-D space.

Fig. 2 illustrates a target and anchor locations in 3-D space. As shown in Fig. 2, $\boldsymbol{x}_i = [x_{i1}, x_{i2}, x_{i3}]^T$ and $\boldsymbol{a}_j = [a_{j1}, a_{j2}, a_{j3}]^T$ are, respectively, the unknown coordinates of the ith target and the known coordinates of the jth anchor, whereas $d_{ij}^{\mathcal{A}}$, $\phi_{ij}^{\mathcal{A}}$, and $\alpha_{ij}^{\mathcal{A}}$ represent the distance, azimuth angle, and elevation angle between the ith target and the jth anchor, respectively. The ML estimate of the distance between two sensors can be obtained from the RSS measurement model (1) as follows [1]:

$$\hat{d}_{ij}^{\mathcal{A}} = d_0 10^{\frac{L_{ij}^{\mathcal{A}} - L_0}{10\gamma}}, \text{ for } (i,j)\in\mathcal{A} \quad (2a)$$

$$\hat{d}_{ik}^{\mathcal{B}} = d_0 10^{\frac{L_{ik}^{\mathcal{B}} - L_0}{10\gamma}}, \text{ for } (i,k)\in\mathcal{B}. \quad (2b)$$

Applying simple geometry, azimuth and elevation angle measurements can be modeled as [25]

$$\phi_{ij}^{\mathcal{A}} = \arctan\left(\frac{x_{i2} - a_{j2}}{x_{i1} - a_{j1}}\right) + m_{ij}, \text{ for } (i,j)\in\mathcal{A} \quad (3a)$$

$$\phi_{ik}^{\mathcal{B}} = \arctan\left(\frac{x_{i2} - x_{k2}}{x_{i1} - x_{k1}}\right) + m_{ik}, \text{ for } (i,k)\in\mathcal{B} \quad (3b)$$

$$\alpha_{ij}^{\mathcal{A}} = \arccos\left(\frac{x_{i3} - a_{j3}}{\|\boldsymbol{x}_i - \boldsymbol{a}_j\|}\right) + v_{ij}, \text{ for } (i,j)\in\mathcal{A} \quad (4a)$$

$$\alpha_{ik}^{\mathcal{B}} = \arccos\left(\frac{x_{i3} - x_{k3}}{\|\boldsymbol{x}_i - \boldsymbol{x}_k\|}\right) + v_{ik}, \text{ for } (i,k)\in\mathcal{B} \quad (4b)$$

respectively, where m_{ij}, m_{ik} and v_{ij}, v_{ik} are, respectively, the measurement errors of azimuth and elevation angles, which are modeled as $m_{ij} \sim \mathcal{N}(0, \sigma^2_{m_{ij}})$, $m_{ik} \sim \mathcal{N}(0, \sigma^2_{m_{ik}})$ and $v_{ij} \sim \mathcal{N}(0, \sigma^2_{v_{ij}})$, $v_{ik} \sim \mathcal{N}(0, \sigma^2_{v_{ik}})$.

Given the observation vector $\boldsymbol{\theta} = [\boldsymbol{L}^T, \boldsymbol{\phi}^T, \boldsymbol{\alpha}^T]^T$ ($\boldsymbol{\theta} \in \mathbb{R}^{3(|\mathcal{A}|+|\mathcal{B}|)}$), where $\boldsymbol{L} = [L^{\mathcal{A}}_{ij}, L^{\mathcal{B}}_{ik}]^T$, $\boldsymbol{\phi} = [\phi^{\mathcal{A}}_{ij}, \phi^{\mathcal{B}}_{ik}]^T$, $\boldsymbol{\alpha} = [\alpha^{\mathcal{A}}_{ij}, \alpha^{\mathcal{B}}_{ik}]^T$, and $|\bullet|$ denotes the cardinality of a set (the number of elements in a set), the conditional probability density function (pdf) is given as

$$p(\boldsymbol{\theta}|\boldsymbol{x}) = \prod_{i=1}^{3(|\mathcal{A}|+|\mathcal{B}|)} \frac{1}{\sqrt{2\pi\sigma_i^2}} \exp\left\{-\frac{(\theta_i - f_i(\boldsymbol{x}))^2}{2\sigma_i^2}\right\} \quad (5)$$

where

$$\boldsymbol{f}(\boldsymbol{x}) = \begin{bmatrix} \vdots \\ L_0 + 10\gamma \log_{10} \frac{\|\boldsymbol{x}_i - \boldsymbol{a}_j\|}{d_0} \\ \vdots \\ L_0 + 10\gamma \log_{10} \frac{\|\boldsymbol{x}_i - \boldsymbol{x}_k\|}{d_0} \\ \vdots \\ \arctan\left(\frac{x_{i2} - a_{j2}}{x_{i1} - a_{j1}}\right) \\ \vdots \\ \arctan\left(\frac{x_{i2} - x_{k2}}{x_{i1} - x_{k1}}\right) \\ \vdots \\ \arccos\left(\frac{x_{i3} - a_{j3}}{\|\boldsymbol{x}_i - \boldsymbol{a}_j\|}\right) \\ \vdots \\ \arccos\left(\frac{x_{i3} - x_{k3}}{\|\boldsymbol{x}_i - \boldsymbol{x}_k\|}\right) \\ \vdots \end{bmatrix}, \ \boldsymbol{\sigma} = \begin{bmatrix} \vdots \\ \sigma_{n_{ij}} \\ \vdots \\ \sigma_{n_{ik}} \\ \vdots \\ \sigma_{m_{ij}} \\ \vdots \\ \sigma_{m_{ik}} \\ \vdots \\ \sigma_{v_{ij}} \\ \vdots \\ \sigma_{v_{ik}} \\ \vdots \end{bmatrix}.$$

The most common estimator used in practice is the ML estimator, since it has the property of being asymptotically efficient (for large enough data records) [37], [38]. The ML estimator forms its estimate as the vector $\hat{\boldsymbol{x}}$, which maximizes the conditional pdf in (5); hence, the ML estimator is obtained as

$$\hat{\boldsymbol{x}} = \underset{\boldsymbol{x}}{\operatorname{argmin}} \sum_{i=1}^{3(|\mathcal{A}|+|\mathcal{B}|)} \frac{1}{\sigma_i^2} \left[\theta_i - f_i(\boldsymbol{x})\right]^2. \quad (6)$$

Although the ML estimator is approximately the minimum-variance unbiased estimator [37], the LS problem in (6) is nonconvex and has no closed-form solution. In the remainder of this work, we will show that the LS problem in (6) can be efficiently solved by applying certain approximations. More precisely, for noncooperative WSNs, we propose a suboptimal estimator based on the GTRS framework leading to an SR-WLS estimator, which can be solved exactly by a bisection procedure [33]. For the case of cooperative WSNs, we propose a convex relaxation technique leading to an SDP estimator that can be efficiently solved by interior-point algorithms [39]. Not only that the new approaches efficiently solve the traditional RSS/AoA localization problem, but they can also be used to solve the localization problem when P_T is not known, with straightforward generalization.

A. Assumptions

We outline here some assumptions for the WSN (made for the sake of simplicity and without loss of generality).

1) The network is connected, and it does not change during the computation time.
2) Measurement errors for the RSS and AoA models are independent, and $\sigma_{n_{ij}} = \sigma_n$, $\sigma_{m_{ij}} = \sigma_m$, and $\sigma_{v_{ij}} = \sigma_v \ \forall \ (i, j) \in \mathcal{A} \cup \mathcal{B}$.
3) The range measurements are extracted from the RSS information exclusively, and all target/target measurements are symmetric.
4) All sensors have identical P_T values.
5) All sensors are equipped with either multiple antennas or a directional antenna, and they can measure the AoA information.

In assumption (1), we assume that the sensors are static and that there is no node/link failure during the computation period, and all sensors can convey their measurements to a central processor. Assumptions (2) and (4) are made for the sake of simplicity. Assumption (3) is made without loss of generality; it is readily seen that if $L^{\mathcal{B}}_{ik} \neq L^{\mathcal{B}}_{ki}$, then it serves to replace $L^{\mathcal{B}}_{ik} \leftarrow (L^{\mathcal{B}}_{ik} + L^{\mathcal{B}}_{ki})/2$ and $L^{\mathcal{B}}_{ki} \leftarrow (L^{\mathcal{B}}_{ik} + L^{\mathcal{B}}_{ki})/2$ when solving the localization problem. Assumption (4) implies that L_0 and R are identical for all sensors. Finally, assumption (5) is made for the case of cooperative localization, where only some targets are able to directly connect to anchors; thus, they are forced to cooperate with other targets within their communication range.

III. Noncooperative Localization

By noncooperative WSN, we imply a network comprising a number of targets and anchors, where each target is allowed to communicate with anchors exclusively, and a single target is localized at a time. For such a setting, we can assume that the targets are passive nodes that only emit radio signals and that all radio measurements are collected by anchors.

In the remainder of this section, we develop a suboptimal estimator to solve the noncooperative localization problem in (6), whose *exact* solution can be obtained by a bisection procedure. We then show that its generalization for the case where P_T is not known is straightforward.

A. Noncooperative Localization With Known P_T

Note that the targets communicate with anchors exclusively in a noncooperative network; hence, the set $\mathcal{B}$ in path-loss model (1) is empty. Therefore, when the noise power is sufficiently small, from (1a), we have

$$\lambda^{\mathcal{A}}_{ij} \|\boldsymbol{x}_i - \boldsymbol{a}_j\| \approx d_0 \ \text{for} \ (i, j) \in \mathcal{A} \quad (7)$$

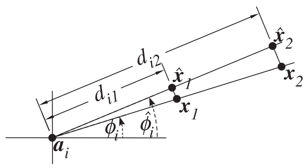

Fig. 3. Illustration of azimuth angle measurements: short-range versus long-range.

where $\lambda_{ij}^{\mathcal{A}} = 10^{(L_0 - L_{ij}^{\mathcal{A}})/10\gamma}$. Similarly, from (3a) and (4a), respectively, we get

$$\boldsymbol{c}_{ij}^T(\boldsymbol{x}_i - \boldsymbol{a}_j) \approx 0 \tag{8}$$

$$\boldsymbol{k}_{ij}^T(\boldsymbol{x}_i - \boldsymbol{a}_j) \approx \|\boldsymbol{x}_i - \boldsymbol{a}_j\| \cos\left(\alpha_{ij}^{\mathcal{A}}\right) \tag{9}$$

where $\boldsymbol{c}_{ij} = [-\sin(\phi_{ij}^{\mathcal{A}}), \cos(\phi_{ij}^{\mathcal{A}}), 0]^T$, and $\boldsymbol{k}_{ij} = [0, 0, 1]^T$.

Next, we can rewrite (7) as

$$\lambda_{ij}^{\mathcal{A}\,2}\|\boldsymbol{x}_i - \boldsymbol{a}_j\|^2 \approx d_0^2. \tag{10}$$

Introduce weights, $\boldsymbol{w} = [\sqrt{w_{ij}}]$, where each w_{ij} is defined as

$$w_{ij} = 1 - \frac{\hat{d}_{ij}^{\mathcal{A}}}{\sum_{(i,j)\in\mathcal{A}} \hat{d}_{ij}^{\mathcal{A}}}$$

such that more importance is given to nearby links. The reason for defining the weights in this manner is because both RSS and AoA short-range measurements are trusted more than long-range measurements. The RSS measurements have relatively constant standard deviation with distance [1]. This implies that multiplicative factors of RSS measurements are constant with range. For example, for a multiplicative factor of 1.5, at a range of 1 m, the measured range would be 1.5 m, and at an actual range of 10 m, the measured range would be 15 m, which is a factor ten times greater [1]. In the case of AoA measurements, the reason is more intuitive, and we call the reader's attention to Fig. 3.

In Fig. 3, an azimuth angle measurement made between an anchor and two targets located along the same line but with different distances from the anchor is illustrated. The true and measured azimuth angles between the anchor and the targets are denoted by ϕ_i and $\hat{\phi}_i$, respectively. Our goal is to determine the locations of the two targets. Based on the available information, the location estimates of the two targets are at points $\hat{\boldsymbol{x}}_1$ and $\hat{\boldsymbol{x}}_2$. However, in Fig. 3, it is shown that the estimated location of the target physically closer to the anchor ($\hat{\boldsymbol{x}}_1$) is much closer to its true location than that further away. In other words, for a given angle, the more two sensors are physically further apart, the greater the set of all possible solutions will be (more likely to impair the localization accuracy).

Replace $\|\boldsymbol{x}_i - \boldsymbol{a}_j\|$ in (9) with $\hat{d}_{ij}^{\mathcal{A}}$ described in (2a), to obtain the following WLS problem according to (8)–(10):

$$\begin{aligned}\hat{\boldsymbol{x}}_i = \underset{\boldsymbol{x}_i}{\arg\min} & \sum_{(i,j):(i,j)\in\mathcal{A}} w_{ij}\left(\lambda_{ij}^{\mathcal{A}\,2}\|\boldsymbol{x}_i - \boldsymbol{a}_j\|^2 - d_0^2\right)^2 \\ & + \sum_{(i,j):(i,j)\in\mathcal{A}} w_{ij}\left(\boldsymbol{c}_{ij}^T(\boldsymbol{x}_i - \boldsymbol{a}_j)\right)^2 \\ & + \sum_{(i,j):(i,j)\in\mathcal{A}} w_{ij}\left(\boldsymbol{k}_{ij}^T(\boldsymbol{x}_i - \boldsymbol{a}_j) - \hat{d}_{ij}^{\mathcal{A}}\cos(\alpha_{ij}^{\mathcal{A}})\right)^2. \end{aligned} \tag{11}$$

The given WLS estimator is nonconvex and has no closed-form solution. However, we can express (11) as a quadratic programming problem whose *global* solution can be efficiently computed [33]. Using the substitution $\boldsymbol{y}_i = [\boldsymbol{x}_i^T, \|\boldsymbol{x}_i\|^2]^T$, the problem in (11) can be rewritten as

$$\underset{\boldsymbol{y}_i}{\text{minimize}} \ \|\boldsymbol{W}(\boldsymbol{A}\boldsymbol{y}_i - \boldsymbol{b})\|^2$$

subject to

$$\boldsymbol{y}_i^T\boldsymbol{D}\boldsymbol{y}_i + 2\boldsymbol{l}^T\boldsymbol{y}_i = 0 \tag{12}$$

where $\boldsymbol{W} = \boldsymbol{I}_3 \otimes \text{diag}(\boldsymbol{w})$

$$\boldsymbol{A} = \begin{bmatrix} \vdots & \vdots \\ -2\lambda_{ij}^{\mathcal{A}\,2}\boldsymbol{a}_j^T & \lambda_{ij}^{\mathcal{A}\,2} \\ \vdots & \vdots \\ \boldsymbol{c}_{ij}^T & 0 \\ \vdots & \vdots \\ \boldsymbol{k}_{ij}^T & 0 \\ \vdots & \vdots \end{bmatrix}, \ \boldsymbol{b} = \begin{bmatrix} \vdots \\ d_0^2 - \lambda_{ij}^{\mathcal{A}\,2}\|\boldsymbol{a}_j\|^2 \\ \vdots \\ \boldsymbol{c}_{ij}^T\boldsymbol{a}_j \\ \vdots \\ \boldsymbol{k}_{ij}^T\boldsymbol{a}_j + \hat{d}_{ij}^{\mathcal{A}}\cos(\alpha_{ij}^{\mathcal{A}}) \\ \vdots \end{bmatrix}$$

$$\boldsymbol{D} = \begin{bmatrix} \boldsymbol{I}_3 & \boldsymbol{0}_{3\times1} \\ \boldsymbol{0}_{1\times3} & 0 \end{bmatrix}, \ \boldsymbol{l} = \begin{bmatrix} \boldsymbol{0}_{3\times1} \\ -1/2 \end{bmatrix}$$

i.e., $\boldsymbol{A} \in \mathbb{R}^{3|\mathcal{A}|\times4}$, $\boldsymbol{b} \in \mathbb{R}^{3|\mathcal{A}|\times1}$, and $\boldsymbol{W} \in \mathbb{R}^{3|\mathcal{A}|\times3|\mathcal{A}|}$.

The objective function and the constraint in (12) are both quadratic. This type of problem is known as GTRS [33], [40], and it can be solved exactly by a bisection procedure [33]. We denote (12) as "SR-WLS1" in the remaining text.

B. Noncooperative Localization With Unknown P_T

To maintain low implementation costs, testing and calibration are not the priority in practice. Thus, sensors' transmit power values are often not calibrated, i.e., not known. Not knowing P_T in the RSS measurement model corresponds to not knowing L_0 in the path-loss model (1) (see [9], [12], and the references therein).

The generalization of the proposed estimators for known L_0 is straightforward for the case where L_0 is not known. Notice that (7) can be rewritten as

$$\beta_{ij}^{\mathcal{A}}\|\boldsymbol{x}_i - \boldsymbol{a}_j\| \approx \eta d_0, \ \text{for } (i,j) \in \mathcal{A} \tag{13}$$

where $\beta_{ij}^{\mathcal{A}} = 10^{-(L_{ij}^{\mathcal{A}}/10\gamma)}$, and $\eta = 10^{-(L_0/10\gamma)}$ is an unknown parameter that needs to be estimated.

Substitute $\|\boldsymbol{x}_i - \boldsymbol{a}_j\|$ with $\hat{d}_{ij}^{\mathcal{A}}$ in (9). Then, we can rewrite (9) as

$$\beta_{ij}^{\mathcal{A}}\boldsymbol{k}_{ij}^T(\boldsymbol{x}_i - \boldsymbol{a}_j) \approx \eta d_0 \cos(\alpha_{ij}^{\mathcal{A}}). \tag{14}$$

To assign more importance to nearby links, introduce weights $\widetilde{\boldsymbol{w}} = [\sqrt{\widetilde{w}_{ij}}]$, where

$$\widetilde{w}_{ij} = 1 - \frac{L_{ij}^{\mathcal{A}}}{\sum_{(i,j)\in\mathcal{A}} L_{ij}^{\mathcal{A}}}.$$

By squaring (13), we can obtain the following WLS problem according to (13), (8), and (14):

$$(\hat{\boldsymbol{x}}_i, \hat{\eta}) = \underset{\boldsymbol{x}_i,\eta}{\operatorname{argmin}} \sum_{(i,j):(i,j)\in\mathcal{A}} \widetilde{w}_{ij}\left({\beta_{ij}^{\mathcal{A}}}^2\|\boldsymbol{x}_i - \boldsymbol{a}_j\|^2 - \eta^2 d_0^2\right)^2 + \sum_{(i,j):(i,j)\in\mathcal{A}} \widetilde{w}_{ij}\left(\boldsymbol{c}_{ij}^T(\boldsymbol{x}_i - \boldsymbol{a}_j)\right)^2 + \sum_{(i,j):(i,j)\in\mathcal{A}} \widetilde{w}_{ij}\left(\beta_{ij}^{\mathcal{A}}\boldsymbol{k}_{ij}^T(\boldsymbol{x}_i - \boldsymbol{a}_j) - \eta d_0\cos(\alpha_{ij}^{\mathcal{A}})\right)^2.$$

Using the substitution $\widetilde{\boldsymbol{y}}_i = [\boldsymbol{x}_i^T, \|\boldsymbol{x}_i\|^2, \eta, \eta^2]^T$, we can rewrite (15) as a GTRS, i.e.,

$$\underset{\widetilde{\boldsymbol{y}}_i}{\operatorname{minimize}} \ \|\widetilde{\boldsymbol{W}}(\widetilde{\boldsymbol{A}}\widetilde{\boldsymbol{y}}_i - \widetilde{\boldsymbol{b}})\|^2$$

subject to

$$\widetilde{\boldsymbol{y}}_i^T\widetilde{\boldsymbol{D}}\widetilde{\boldsymbol{y}}_i + 2\widetilde{\boldsymbol{l}}^T\widetilde{\boldsymbol{y}}_i = 0 \tag{15}$$

where $\widetilde{\boldsymbol{W}} = \boldsymbol{I}_3 \otimes \operatorname{diag}(\widetilde{\boldsymbol{w}})$, $\widetilde{\boldsymbol{D}} = \operatorname{diag}([1,1,1,0,1,0])$, and

$$\widetilde{\boldsymbol{A}} = \begin{bmatrix} \vdots & \vdots & \vdots & \vdots \\ -2{\beta_{ij}^{\mathcal{A}}}^2\boldsymbol{a}_j^T & {\beta_{ij}^{\mathcal{A}}}^2 & 0 & -d_0 \\ \vdots & \vdots & \vdots & \vdots \\ \boldsymbol{c}_{ij}^T & 0 & 0 & 0 \\ \vdots & \vdots & \vdots & \vdots \\ \beta_{ij}^{\mathcal{A}}\boldsymbol{k}_{ij}^T & 0 & -d_0\cos(\alpha_{ij}^{\mathcal{A}}) & 0 \\ \vdots & \vdots & \vdots & \vdots \end{bmatrix}$$

$$\widetilde{\boldsymbol{b}} = \begin{bmatrix} \vdots \\ -{\beta_{ij}^{\mathcal{A}}}^2\|\boldsymbol{a}_j\|^2 \\ \vdots \\ \boldsymbol{c}_{ij}^T\boldsymbol{a}_j \\ \vdots \\ \beta_{ij}^{\mathcal{A}}\boldsymbol{k}_{ij}^T\boldsymbol{a}_j \\ \vdots \end{bmatrix}$$

$$\widetilde{\boldsymbol{l}} = \left[\boldsymbol{0}_{1\times 3},\ -\frac{1}{2},\ 0,\ -\frac{1}{2}\right]^T$$

i.e., $\widetilde{\boldsymbol{A}} \in \mathbb{R}^{3|\mathcal{A}|\times 6}$, $\widetilde{\boldsymbol{b}} \in \mathbb{R}^{3|\mathcal{A}|\times 1}$, and $\widetilde{\boldsymbol{W}} \in \mathbb{R}^{3|\mathcal{A}|\times 3|\mathcal{A}|}$.

Although the approach in (15) efficiently solves (6) for unknown L_0, we can further improve its performance. To do so, we will first solve (15) to obtain the location estimate and use this estimate to find the ML estimate of L_0, i.e., $\widehat{L}_0$. Then, we will take advantage of $\widehat{L}_0$ to solve another WLS problem as if L_0 is known. Hence, the proposed procedure for solving (6) when L_0 is not known is summarized as follows.

1) Solve (15) to obtain the initial estimate of $\boldsymbol{x}_i$, $\hat{\boldsymbol{x}}_i'$.
2) Use $\hat{\boldsymbol{x}}_i'$ to compute the ML estimate of L_0, $\widehat{L}_0$ as

$$\widehat{L}_0 = \frac{\sum_{(i,j)\in\mathcal{A}}\left(L_{ij}^{\mathcal{A}} - 10\gamma\log_{10}\frac{\|\hat{\boldsymbol{x}}_i' - \boldsymbol{a}_j\|}{d_0}\right)}{|\mathcal{A}|}.$$

3) Exploit $\widehat{L}_0$ to calculate $\hat{\lambda}_{ij}^{\mathcal{A}} = 10^{(\widehat{L}_0 - L_{ij}^{\mathcal{A}})/10\gamma}$ and use this estimated value to solve the SR-WLS in (12).

The main reason for applying this simple procedure is that we observed in our simulations that after solving (15), an excellent ML estimation of L_0, i.e., $\widehat{L}_0$, is obtained, which is very close to the true value of L_0. This motivated us to take advantage of this estimated value to solve another WLS problem (12), as if L_0 is known. We denote the given three-step procedure as "SR-WLS2" in the remaining text.

IV. Cooperative Localization

By cooperative WSN, we imply a network consisting of a number of targets and anchors, where a target can communicate with any sensor within its communication range, and all targets are simultaneously localized. A kind of node cooperation is required in networks with modest energy capabilities, where communication ranges are limited (to prolong the sensors' battery lives), and only some targets can directly communicate with the anchor nodes.

Throughout this section, we develop a convex estimator by using an appropriate relaxation technique leading to an SDP estimator for 3-D localization. Moreover, we show that the generalization of the proposed estimator to the case of unknown L_0 is straightforward.

For sufficiently small noise, (1), (3), and (4) can be rewritten as

$${\lambda_{ij}^{\mathcal{A}}}^2\|\boldsymbol{x}_i - \boldsymbol{a}_j\|^2 \approx d_0^2, \text{ for } (i,j)\in\mathcal{A} \tag{16a}$$

$${\lambda_{ik}^{\mathcal{B}}}^2\|\boldsymbol{x}_i - \boldsymbol{x}_k\|^2 \approx d_0^2, \text{ for } (i,k)\in\mathcal{B} \tag{16b}$$

$$\boldsymbol{c}_{ij}^T(\boldsymbol{x}_i - \boldsymbol{a}_j) \approx 0, \quad \text{for } (i,j)\in\mathcal{A} \tag{17a}$$

$$\boldsymbol{c}_{ik}^T(\boldsymbol{x}_i - \boldsymbol{x}_k) \approx 0, \quad \text{for } (i,k)\in\mathcal{B} \tag{17b}$$

$$\boldsymbol{k}_{ij}^T(\boldsymbol{x}_i - \boldsymbol{a}_j)(\boldsymbol{x}_i - \boldsymbol{a}_j)^T\boldsymbol{k}_{ij} \approx \|\boldsymbol{x}_i - \boldsymbol{a}_j\|^2\cos^2(\alpha_{ij}^{\mathcal{A}}), \quad \text{for } (i,j)\in\mathcal{A} \tag{18a}$$

$$\boldsymbol{k}_{ik}^T(\boldsymbol{x}_i - \boldsymbol{x}_k)(\boldsymbol{x}_i - \boldsymbol{x}_k)^T\boldsymbol{k}_{ik} \approx \|\boldsymbol{x}_i - \boldsymbol{x}_k\|^2\cos^2(\alpha_{ik}^{\mathcal{B}}), \quad \text{for } (i,k)\in\mathcal{B} \tag{18b}$$

where $\lambda_{ik}^{\mathcal{B}} = 10^{(L_0 - L_{ik}^{\mathcal{B}})/10\gamma}$, $\boldsymbol{c}_{ik} = [-\sin(\phi_{ik}^{\mathcal{B}}), \cos(\phi_{ik}^{\mathcal{B}}), 0]^T$, and $\boldsymbol{k}_{ik} = [0,0,1]^T$.

Following the LS principle, from (16)–(18), we obtain the target location estimates, $\hat{\boldsymbol{x}}$, by minimizing the objective function, i.e.,

$$\begin{aligned}\hat{\boldsymbol{x}} = \underset{\boldsymbol{x}}{\operatorname{argmin}} & \sum_{(i,j):(i,j)\in\mathcal{A}} \left(\lambda_{ij}^{\mathcal{A}\,2}\|\boldsymbol{x}_i-\boldsymbol{a}_j\|^2-d_0^2\right)^2 \\ & + \sum_{(i,j):(i,j)\in\mathcal{A}} \left(\boldsymbol{c}_{ij}^T\left(\boldsymbol{x}_i-\boldsymbol{a}_j\right)\right)^2 \\ & + \sum_{(i,j):(i,j)\in\mathcal{A}} \Big(\boldsymbol{k}_{ij}^T\left(\boldsymbol{x}_i-\boldsymbol{a}_j\right)\left(\boldsymbol{x}_i-\boldsymbol{a}_j\right)^T\boldsymbol{k}_{ij} \\ & \qquad -\|\boldsymbol{x}_i-\boldsymbol{a}_j\|^2\cos^2\left(\alpha_{ij}^{\mathcal{A}}\right)\Big)^2 \\ & + \sum_{(i,k):(i,k)\in\mathcal{B}} \left(\lambda_{ik}^{\mathcal{B}\,2}\|\boldsymbol{x}_i-\boldsymbol{x}_k\|^2-d_0^2\right)^2 \\ & + \sum_{(i,k):(i,k)\in\mathcal{B}} \left(\boldsymbol{c}_{ik}^T\left(\boldsymbol{x}_i-\boldsymbol{x}_k\right)\right)^2 \\ & + \sum_{(i,k):(i,k)\in\mathcal{B}} \Big(\boldsymbol{k}_{ik}^T\left(\boldsymbol{x}_i-\boldsymbol{x}_k\right)\left(\boldsymbol{x}_i-\boldsymbol{x}_k\right)^T\boldsymbol{k}_{ik} \\ & \qquad -\|\boldsymbol{x}_i-\boldsymbol{x}_k\|^2\cos^2\left(\alpha_{ik}^{\mathcal{B}}\right)\Big)^2. \end{aligned} \tag{19}$$

Although the optimization problem in (19) is nonconvex and has no closed-form solution, we will show in the following text that it can be converted into an SDP problem.

A. Cooperative Localization With Known P_T

A common approach in the literature (when dealing with cooperative localization) is to stack all unknowns in one big matrix variable $\boldsymbol{Y}=[\boldsymbol{x}_1,\ldots,\boldsymbol{x}_M]$ ($\boldsymbol{Y}\in\mathbb{R}^{3\times M}$) [17]–[20]. However, this approach cannot be applied to solving (19) because of the vector outer product that appears in two sums with respect to the elevation angle. Instead, we assemble the unknowns in a vector, which allows us to cope effortlessly with the outer product.

Introduce auxiliary variable $\boldsymbol{X}=\boldsymbol{x}\boldsymbol{x}^T$ ($\boldsymbol{X}\in\mathbb{R}^{3M\times 3M}$). Moreover, introduce an auxiliary vector $\boldsymbol{z}=[z_{ij}^{\mathcal{A}},g_{ij}^{\mathcal{A}},p_{ij}^{\mathcal{A}},z_{ik}^{\mathcal{B}},g_{ik}^{\mathcal{B}},p_{ik}^{\mathcal{B}}]^T$ ($\boldsymbol{z}\in\mathbb{R}^{3(|\mathcal{A}|+|\mathcal{B}|)\times 1}$). Then, the problem in (19) can be rewritten as

$$\underset{\boldsymbol{x},\boldsymbol{X},\boldsymbol{z}}{\text{minimize}}\ \|\boldsymbol{z}\|^2$$

subject to

$$z_{ij}^{\mathcal{A}} = \lambda_{ij}^{\mathcal{A}\,2}\left(\operatorname{tr}\left(\boldsymbol{E}_i^T\boldsymbol{X}\boldsymbol{E}_i\right)-2\boldsymbol{a}_j^T\boldsymbol{E}_i^T\boldsymbol{x}+\|\boldsymbol{a}_j\|^2\right)-d_0^2 \tag{20a}$$

$$g_{ij}^{\mathcal{A}} = \boldsymbol{c}_{ij}^T\left(\boldsymbol{E}_i^T\boldsymbol{x}-\boldsymbol{a}_j\right),\ \text{for } (i,j)\in\mathcal{A} \tag{20b}$$

$$\begin{aligned} p_{ij}^{\mathcal{A}} &= \boldsymbol{k}_{ij}^T\left(\boldsymbol{E}_i^T\boldsymbol{X}\boldsymbol{E}_i-2\boldsymbol{E}_i^T\boldsymbol{x}\boldsymbol{a}_j^T+\boldsymbol{a}_j\boldsymbol{a}_j^T\right)\boldsymbol{k}_{ij} \\ &\quad -\left(\operatorname{tr}\left(\boldsymbol{E}_i^T\boldsymbol{X}\boldsymbol{E}_i\right)-2\boldsymbol{a}_j^T\boldsymbol{E}_i^T\boldsymbol{x}+\|\boldsymbol{a}_j\|^2\right)\cos^2(\alpha_{ij}^{\mathcal{A}}) \end{aligned} \tag{20c}$$

$$\begin{aligned} z_{ik}^{\mathcal{B}} &= \lambda_{ik}^{\mathcal{B}\,2}\left(\operatorname{tr}\left(\boldsymbol{E}_i^T\boldsymbol{X}\boldsymbol{E}_i\right)-2\operatorname{tr}\left(\boldsymbol{E}_i^T\boldsymbol{X}\boldsymbol{E}_k\right)\right. \\ &\qquad \left.+\operatorname{tr}\left(\boldsymbol{E}_{\boldsymbol{k}}^T\boldsymbol{X}\boldsymbol{E}_{\boldsymbol{k}}\right)\right)-d_0^2 \end{aligned} \tag{20d}$$

$$g_{ik}^{\mathcal{B}} = \boldsymbol{c}_{ik}^T\left(\boldsymbol{E}_i^T\boldsymbol{x}-\boldsymbol{E}_k^T\boldsymbol{x}\right),\ \text{for } (i,k)\in\mathcal{B} \tag{20e}$$

$$\begin{aligned} p_{ik}^{\mathcal{B}} &= \boldsymbol{k}_{ik}^T\left(\boldsymbol{E}_i^T\boldsymbol{X}\boldsymbol{E}_i-2\boldsymbol{E}_i^T\boldsymbol{X}\boldsymbol{E}_k+\boldsymbol{E}_k^T\boldsymbol{X}\boldsymbol{E}_k\right)\boldsymbol{k}_{ik} \\ &\quad -\left(\operatorname{tr}\left(\boldsymbol{E}_i^T\boldsymbol{X}\boldsymbol{E}_i\right)-2\operatorname{tr}\left(\boldsymbol{E}_i^T\boldsymbol{X}\boldsymbol{E}_k\right)\right. \\ &\qquad \left.+\operatorname{tr}\left(\boldsymbol{E}_k^T\boldsymbol{X}\boldsymbol{E}_k\right)\right)\cos^2(\alpha_{ik}^{\mathcal{B}}) \end{aligned} \tag{20f}$$

$$\boldsymbol{X}=\boldsymbol{x}\boldsymbol{x}^T. \tag{20g}$$

Defining an epigraph variable, i.e., t, together with the semidefinite and second-order cone (SOC) relaxations of the form $\boldsymbol{X}\succeq\boldsymbol{x}\boldsymbol{x}^T$ and $\|\boldsymbol{z}\|^2\le t$, respectively, the following convex epigraph form is obtained from the given problem:

$$\underset{\boldsymbol{x},\boldsymbol{X},\boldsymbol{z},t}{\text{minimize}}\ t$$

subject to (20a)–(20f)

$$\left\|\begin{bmatrix}2\boldsymbol{z}\\ t-1\end{bmatrix}\right\|\le t+1,\ \begin{bmatrix}\boldsymbol{X} & \boldsymbol{x}\\ \boldsymbol{x}^T & 1\end{bmatrix}\succeq\boldsymbol{0}_{3M+1}. \tag{21}$$

The given problem is an SDP (more precisely, it is a mixed SDP/SOCP), which can be readily solved by CVX [41]. It is worth mentioning that if $\operatorname{rank}(\boldsymbol{X})=1$, then the relaxed constraint $\boldsymbol{X}\succeq\boldsymbol{x}\boldsymbol{x}^T$ is satisfied as an equality [39]. Note also that we applied the Schur complement to rewrite $\boldsymbol{X}\succeq\boldsymbol{x}\boldsymbol{x}^T$ into a semidefinite cone (SDC) constraint form. In the following text, we will denote (21) as "SDP1."

B. Cooperative Localization With Unknown P_T

The generalization of the proposed SDP estimator for known L_0 is straightforward for the case where L_0 is not known. From (16), we have that

$$\beta_{ij}^{\mathcal{A}\,2}\|\boldsymbol{x}_i-\boldsymbol{a}_j\|^2\approx\rho d_0^2,\ \text{for } (i,j)\in\mathcal{A} \tag{22a}$$

$$\beta_{ik}^{\mathcal{B}\,2}\|\boldsymbol{x}_i-\boldsymbol{x}_k\|^2\approx\rho d_0^2,\ \text{for } (i,k)\in\mathcal{B} \tag{22b}$$

where $\beta_{ik}=10^{-(L_{ik}^{\mathcal{B}}/10\gamma)}$ for $(i,k)\in\mathcal{B}$, and $\rho=10^{-(L_0/5\gamma)}$. Therefore, according to (17), (18), and (22), the target location estimates are obtained by minimizing the following LS problem:

$$\begin{aligned}(\hat{\boldsymbol{x}},\hat{\rho}) = \underset{\boldsymbol{x},\rho}{\operatorname{argmin}} & \sum_{(i,j):(i,j)\in\mathcal{A}} \left(\beta_{ij}^{\mathcal{A}\,2}\|\boldsymbol{x}_i-\boldsymbol{a}_j\|^2-\rho d_0^2\right)^2 \\ & + \sum_{(i,j):(i,j)\in\mathcal{A}} \left(\boldsymbol{c}_{ij}^T\left(\boldsymbol{x}_i-\boldsymbol{a}_j\right)\right)^2 \\ & + \sum_{(i,j):(i,j)\in\mathcal{A}} \Big(\boldsymbol{k}_{ij}^T\left(\boldsymbol{x}_i-\boldsymbol{a}_j\right)\left(\boldsymbol{x}_i-\boldsymbol{a}_j\right)^T\boldsymbol{k}_{ij} \\ & \qquad -\|\boldsymbol{x}_i-\boldsymbol{a}_j\|^2\cos^2\left(\alpha_{ij}^{\mathcal{A}}\right)\Big)^2 \\ & + \sum_{(i,k):(i,k)\in\mathcal{B}} \left(\beta_{ik}^{\mathcal{B}\,2}\|\boldsymbol{x}_i-\boldsymbol{x}_k\|^2-\rho d_0^2\right)^2 \\ & + \sum_{(i,k):(i,k)\in\mathcal{B}} \left(\boldsymbol{c}_{ik}^T\left(\boldsymbol{x}_i-\boldsymbol{x}_k\right)\right)^2 \\ & + \sum_{(i,k):(i,k)\in\mathcal{B}} \Big(\boldsymbol{k}_{ik}^T\left(\boldsymbol{x}_i-\boldsymbol{x}_k\right)\left(\boldsymbol{x}_i-\boldsymbol{x}_k\right)^T\boldsymbol{k}_{ik} \\ & \qquad -\|\boldsymbol{x}_i-\boldsymbol{x}_k\|^2\cos^2\left(\alpha_{ik}^{\mathcal{B}}\right)\Big)^2. \end{aligned} \tag{23}$$

By following similar steps as described in Section IV-A, we obtain the SDP estimator defined as follows:

$$\underset{\boldsymbol{x},\rho,\boldsymbol{X},\boldsymbol{z},t}{\text{minimize}}\ t$$

subject to

$$\begin{aligned}
z_{ij}^{\mathcal{A}} &= {\beta_{ij}^{\mathcal{A}}}^2 \left(\mathrm{tr}\left(\boldsymbol{E}_i^T\boldsymbol{X}\boldsymbol{E}_i\right) - 2\boldsymbol{a}_j^T\boldsymbol{E}_i^T\boldsymbol{x} + \|\boldsymbol{a}_j\|^2\right) - \rho d_0^2\\
g_{ij}^{\mathcal{A}} &= \boldsymbol{c}_{ij}^T\left(\boldsymbol{E}_i^T\boldsymbol{x} - \boldsymbol{a}_j\right),\ \text{for } (i,j)\in\mathcal{A}\\
p_{ij}^{\mathcal{A}} &= \boldsymbol{k}_{ij}^T\left(\boldsymbol{E}_i^T\boldsymbol{X}\boldsymbol{E}_i - 2\boldsymbol{E}_i^T\boldsymbol{x}\boldsymbol{a}_j^T + \boldsymbol{a}_j\boldsymbol{a}_j^T\right)\boldsymbol{k}_{ij}\\
&\quad - \left(\mathrm{tr}\left(\boldsymbol{E}_i^T\boldsymbol{X}\boldsymbol{E}_i\right) - 2\boldsymbol{a}_j^T\boldsymbol{E}_i^T\boldsymbol{x} + \|\boldsymbol{a}_j\|^2\right)\cos^2(\alpha_{ij}^{\mathcal{A}})\\
z_{ik}^{\mathcal{B}} &= {\beta_{ik}^{\mathcal{B}}}^2\left(\mathrm{tr}\left(\boldsymbol{E}_i^T\boldsymbol{X}\boldsymbol{E}_i\right) - 2\ \mathrm{tr}\left(\boldsymbol{E}_i^T\boldsymbol{X}\boldsymbol{E}_k\right)\right.\\
&\quad \left. + \mathrm{tr}\left(\boldsymbol{E}_{\boldsymbol{k}}^{\boldsymbol{T}}\boldsymbol{X}\boldsymbol{E}_{\boldsymbol{k}}\right)\right) - \rho d_0^2\\
g_{ik}^{\mathcal{B}} &= \boldsymbol{c}_{ik}^T\left(\boldsymbol{E}_i^T\boldsymbol{x} - \boldsymbol{E}_k^T\boldsymbol{x}\right),\ \text{for } (i,k)\in\mathcal{B}\\
p_{ik}^{\mathcal{B}} &= \boldsymbol{k}_{ik}^T\left(\boldsymbol{E}_i^T\boldsymbol{X}\boldsymbol{E}_i - 2\boldsymbol{E}_i^T\boldsymbol{X}\boldsymbol{E}_k + \boldsymbol{E}_k^T\boldsymbol{X}\boldsymbol{E}_k\right)\boldsymbol{k}_{ik}\\
&\quad - \left(\mathrm{tr}\left(\boldsymbol{E}_i^T\boldsymbol{X}\boldsymbol{E}_i\right) - 2\ \mathrm{tr}\left(\boldsymbol{E}_i^T\boldsymbol{X}\boldsymbol{E}_k\right)\right.\\
&\quad \left. + \mathrm{tr}\left(\boldsymbol{E}_k^T\boldsymbol{X}\boldsymbol{E}_k\right)\right)\cos^2(\alpha_{ik}^{\mathcal{B}}),\\
&\left\|\begin{bmatrix}2\boldsymbol{z}\\ t-1\end{bmatrix}\right\| \le t+1,\ \begin{bmatrix}\boldsymbol{X} & \boldsymbol{x}\\ \boldsymbol{x}^T & 1\end{bmatrix} \succeq \boldsymbol{0}_{3M+1}.
\end{aligned} \tag{24}$$

Although the given SDP estimator efficiently solves the target localization problem for the case of unknown L_0 in a cooperative WSN, we propose the following three-step procedure to further enhance the estimation accuracy.

1) Solve (24) to obtain the initial estimate of all target locations $\boldsymbol{x}$, $\hat{\boldsymbol{x}}'$.
2) Use $\hat{\boldsymbol{x}}'$ to compute the ML estimate of L_0, $\widehat{L}_0$ as

$$\widehat{L}_0 = \frac{\sum_{(i,j):(i,j)\in\mathcal{A}}\left(L_{ij}^{\mathcal{A}} - 10\gamma\log_{10}\frac{\|\boldsymbol{E}_i^T\hat{\boldsymbol{x}}' - \boldsymbol{a}_j\|}{d_0}\right)}{|\mathcal{A}| + |\mathcal{B}|} + \frac{\sum_{(i,k):(i,k)\in\mathcal{B}}\left(L_{ik}^{\mathcal{B}} - 10\gamma\log_{10}\frac{\|\boldsymbol{E}_i^T\hat{\boldsymbol{x}}' - \boldsymbol{E}_k^T\hat{\boldsymbol{x}}'\|}{d_0}\right)}{|\mathcal{A}| + |\mathcal{B}|}.$$

3) Exploit $\widehat{L}_0$ to calculate $\hat{\lambda}_{ij}^{\mathcal{A}} = 10^{(\widehat{L}_0 - L_{ij}^{\mathcal{A}})/10\gamma}$ $\forall\,(i,j)\in\mathcal{A}$ and $\hat{\lambda}_{ik}^{\mathcal{B}} = 10^{(\widehat{L}_0 - L_{ik}^{\mathcal{B}})/10\gamma}$ $\forall\,(i,k)\in\mathcal{B}$ and use these estimated values to solve the SDP in (21) as if L_0 is known.

We refer to the given three-step procedure as "SDP2" in the following text.

V. Complexity Analysis

The tradeoff between estimation accuracy and computational complexity is one of the most important features of any algorithm since it defines its applicability potential. This is why, apart from performance, we also want to analyze the computational complexity of the considered approaches.

The following formula for computing the worst case computational complexity of a mixed SDP/SOCP [42] is used to analyze the complexities of the considered algorithms in this paper:

$$\mathcal{O}\left(\sqrt{L}\left(m\sum_{i=1}^{N_{\mathrm{sd}}} n_i^{\mathrm{sd}^3} + m^2\sum_{i=1}^{N_{\mathrm{sd}}} n_i^{\mathrm{sd}^2} + m^2\sum_{i=1}^{N_{\mathrm{soc}}} n_i^{\mathrm{soc}} + \sum_{i=1}^{N_{\mathrm{soc}}} n_i^{\mathrm{soc}^2} + m^3\right)\right) \tag{25}$$

where L is the iteration complexity of the algorithm; m is the number of equality constraints; n_i^{sd} and n_i^{soc} are, respectively, the dimensions of the ith SDC and the ith SOC; and N_i^{sd} and N_i^{soc} are the number of SDC and SOC constraints, respectively. Equation (25) corresponds to the formula for computing the complexity of an SDP for the case when we have no SOCCs (in which case, L is the dimension of the SDC given as a result of accumulating all SDCs), and *vice versa* (in which case, L is the total number of SOC constraints) [42].

Since we are interested in analyzing the worst case asymptotic computational complexity, we present only the dominating elements, which are expressed as a function of N and M. Therefore, we assume that the network is fully connected,[1] i.e., the total number of connections in the network is $C = |\mathcal{A}| + |\mathcal{B}|$, where $|\mathcal{A}| = MN$, and $|\mathcal{B}| = M(M-1)/2$. In the case of noncooperative localization, each target is located at a time; hence, we can presume that $M = 1$ in this case.

Assuming that $K_{\max}$ is the maximum number of steps in the bisection procedure used to solve (12) and (15), Table I provides an overview of the considered algorithms together with their worst case computational complexity.

Table I reveals that the computational complexity of the considered approaches depends mainly on the network size, i.e., the total number of sensors in the WSN. This property is consistent for algorithms executed in a centralized manner [10], where the acquired information is conveyed to a central processor that performs the necessary computations. As shown in Table I, in the case of noncooperative localization, the proposed estimators based on the GTRS framework are slightly more complex than the existing estimator due to the iterative bisection procedure. However, the higher computational complexity of the proposed estimators is justified by their superior performance in the sense of estimation accuracy, as we will see in Section VI. Finally, in Table I, we can see that the proposed estimators for cooperative localization are computationally the most demanding. This is not surprising, since the cooperative localization problem is very challenging and requires the use of sophisticated mathematical tools to be solved globally.

VI. Performance Results

Here, we present a set of performance results to compare the proposed approaches with the existing approaches, for

[1] In practice, however, the number of connections in the network is significantly smaller, due to energy restrictions, i.e., limited R.

TABLE I
SUMMARY OF THE CONSIDERED ALGORITHMS

Algorithm	Description	Complexity
SR-WLS1	The proposed SR-WLS estimator for non-cooperative localization when P_T is known in Section (12)	$\mathcal{O}\left(K_{\max} N\right)$
LS	The LS estimator for non-cooperative localization when P_T is known in [25]	$\mathcal{O}\left(N\right)$
SR-WLS2	The proposed SR-WLS approach for non-cooperative localization when P_T is unknown in Section III-B	$2\,\mathcal{O}\left(K_{\max} N\right)$
SDP1	The proposed SDP estimator for cooperative localization when P_T is known in (21)	$\mathcal{O}\left(\sqrt{3M}\left(81M^4\left(N+\frac{M}{2}\right)^2\right)\right)$
SDP2	The proposed SDP approach for cooperative localization when P_T is unknown in Section IV-B	$2\mathcal{O}\left(\sqrt{3M}\left(81M^4\left(N+\frac{M}{2}\right)^2\right)\right)$

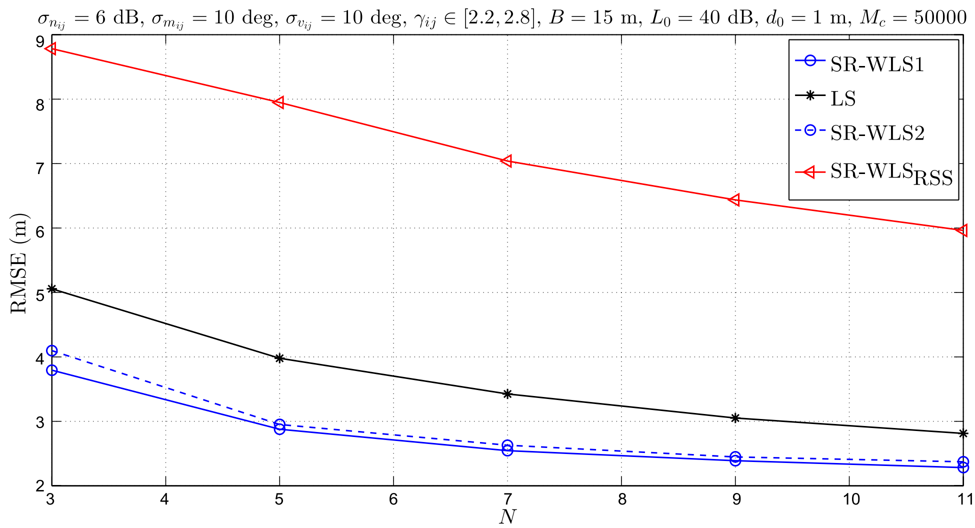

Fig. 4. RMSE-versus-N comparison, when $\sigma_{n_{ij}} = 6$ dB, $\sigma_{m_{ij}} = 10$ deg, $\sigma_{v_{ij}} = 10$ deg, $\gamma_{ij} \in [2.2, 2.8]$, $\gamma = 2.5$, $B = 15$ m, $L_0 = 40$ dB, $d_0 = 1$ m, and $M_c = 50\,000$.

both noncooperative and cooperative localization with known and unknown P_T. To demonstrate the benefit of fusing two radio measurements versus traditional localization systems, we present also the performance results of the proposed methods for known P_T when only RSS measurements are employed, called here SR-WLS$_{\text{RSS}}$ and SDP$_{\text{RSS}}$ for noncooperative and cooperative localization, respectively. Moreover, it is worth mentioning that for the sake of fairness, the range measurements for the LS method in [25] were acquired according to (2a). All of the presented algorithms were solved by using the MATLAB package `CVX` [41], where the solver is SeDuMi [43].

To generate the radio measurements, (1), (3), and (4) were used. We considered a random deployment of nodes inside a box with a length of the edges $B = 15$ m in each Monte Carlo (M_c) run. Random deployment of nodes is of practical interest, since the algorithms are tested against various network topologies. Unless stated otherwise, the reference distance is set to $d_0 = 1$ m, the reference path loss to $L_0 = 40$ dB, the maximum number of steps in the bisection procedure to $K_{\max} = 30$, and the PLE to $\gamma = 2.5$. However, in practice, it is almost impossible to perfectly estimate the value of the PLE. Therefore, to account for a realistic measurement model mismatch and test the robustness of the considered approaches to imperfect knowledge of the PLE, the true PLE for each link was drawn from a uniform distribution on an interval [2.2, 2.8], i.e., $\gamma_{ij} \in [2.2, 2.8]\ \forall\,(i,j) \in \mathcal{A} \cup \mathcal{B}, i \neq j$.

A. Noncooperative WSN

In a noncooperative WSN, targets exclusively communicate with anchors, and one target is located at a time; hence, without loss of generality, we can assume that $M = 1$. It was assumed that the RSS and AoA measurements were performed by anchors. As the main performance metric for noncooperative localization, we used the root mean square error (RMSE) defined as

$$\text{RMSE} = \sqrt{\sum_{i=1}^{M_c} \frac{\|\boldsymbol{x}_i - \widehat{\boldsymbol{x}}_i\|^2}{M_c}}$$

where $\widehat{\boldsymbol{x}}_i$ denotes the estimate of the true target location, i.e., $\boldsymbol{x}_i$, in the ith M_c run.

Fig. 4 shows the RMSE-versus-N comparison when $\sigma_{n_{ij}} = 6$ dB, $\sigma_{m_{ij}} = 10$ deg, and $\sigma_{v_{ij}} = 10$ deg. As anticipated, Fig. 4 reveals that the performance of all algorithms improves as more anchors are added into the network, i.e., as more reliable information is available. It also confirms the effectiveness of using the combined measurements in hybrid systems versus using only a single measurement as in traditional systems. Furthermore, one can see that the proposed estimators for both known and unknown P_T significantly outperform the existing estimator for all N values. Additionally, it can be seen that "SR-WLS2" achieves the lower bound provided by its complement for known P_T, i.e., "SR-WLS1." We can also observe

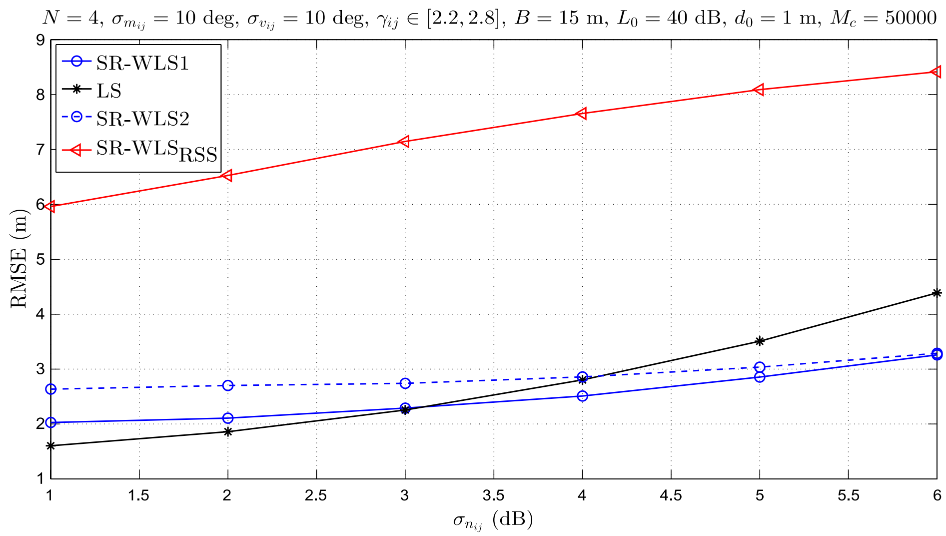

Fig. 5. RMSE-versus-$\sigma_{n_{ij}}$ (dB) comparison, when $N = 4$, $\sigma_{m_{ij}} = 10$ deg, $\sigma_{v_{ij}} = 10$ deg, $\gamma_{ij} \in [2.2, 2.8]$, $\gamma = 2.5$, $B = 15$ m, $L_0 = 40$ dB, $d_0 = 1$ m, and $M_c = 50\,000$.

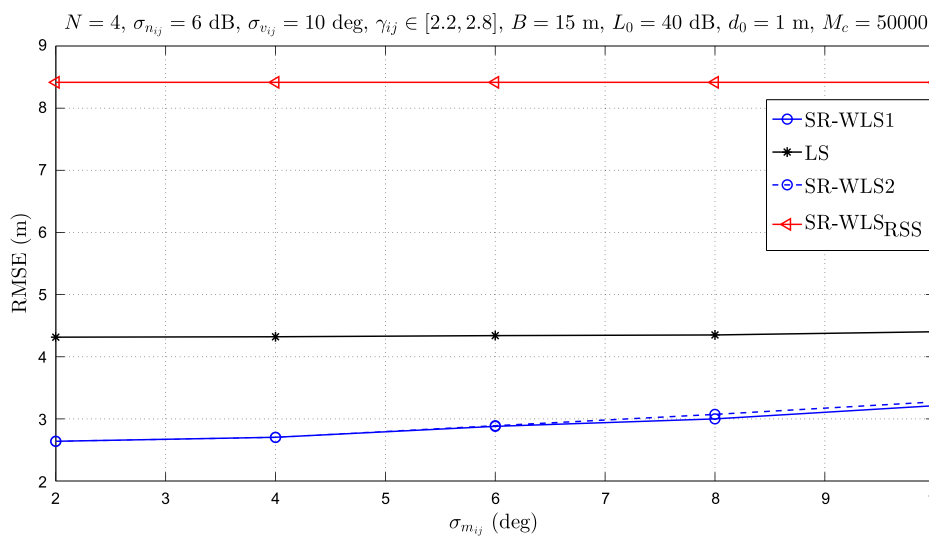

Fig. 6. RMSE-versus-$\sigma_{m_{ij}}$ (deg) comparison, when $N = 4$, $\sigma_{n_{ij}} = 6$ dB, $\sigma_{v_{ij}} = 10$ deg, $\gamma_{ij} \in [2.2, 2.8]$, $\gamma = 2.5$, $B = 15$ m, $L_0 = 40$ dB, $d_0 = 1$ m, and $M_c = 50\,000$.

that the performance margin between the proposed estimators for known and unknown P_T decreases with the increase of N. This behavior is intuitive, since with increased N, we expect to obtain a better estimation of P_T (*closer* to its true value), which would allow us to enhance the estimation accuracy in the third step of our proposed procedure. Finally, although our estimators were based on the assumption that the noise is small, Fig. 4 reveals that they work excellent, even for the cases in which the noise power is high.

In Figs. 5–7, we investigate the influence of the quality of certain types of measurements on the performance of the considered approaches. More specifically, Figs. 5–7 show the RMSE versus $\sigma_{n_{ij}}$ (dB), $\sigma_{m_{ij}}$ (deg), and $\sigma_{v_{ij}}$ (deg) comparison when $N = 4$, respectively. In these figures, one can observe that when the quality of a certain measurement drops, the performance of the considered algorithms worsens, as expected. Furthermore, one can see that both the proposed and the existing approach suffer the biggest deterioration in the performance when the quality of the RSS measurements weakens. Moreover, while the quality of the azimuth angle measurements affect more the proposed approaches than the "LS" method, the error in the elevation angle measurements has very little effect on their performance. Furthermore, it can be seen that the proposed procedure for unknown P_T is robust to the noise feature, since the performance margin between "SR-WLS1" and its counterpart for unknown P_T remains constant with the increase in noise, in general. Finally, Figs. 5–7 exhibit superior performance of the proposed algorithms in comparison with the existing algorithm, in general.

B. *Cooperative WSN*

This section presents the simulation results for the cooperative localization problem. As previously mentioned, to the best of the authors' knowledge, localization algorithms for hybrid RSS/AoA systems in cooperative 3-D WSNs are not

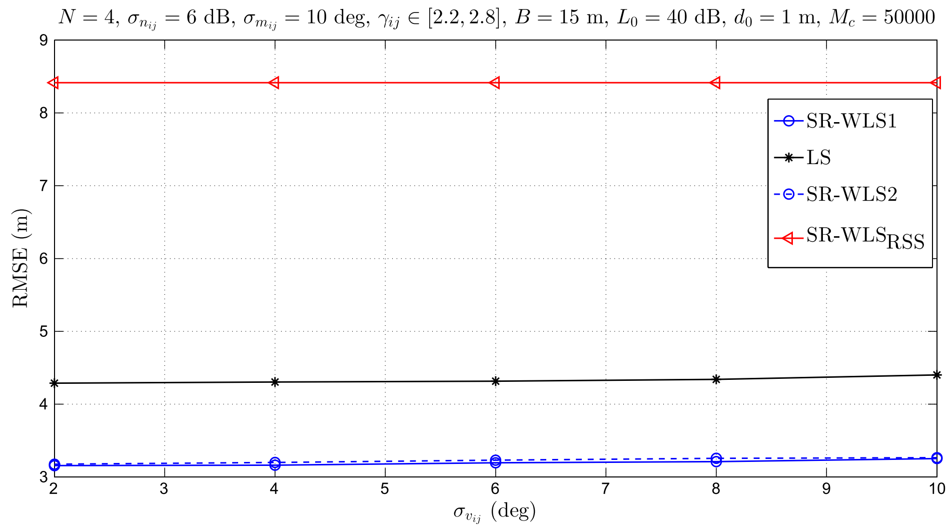

Fig. 7. RMSE-versus-$\sigma_{v_{ij}}$ (deg) comparison, when $N = 4$, $\sigma_{n_{ij}} = 6$ dB, $\sigma_{m_{ij}} = 10$ deg, $\gamma_{ij} \in [2.2, 2.8]$, $\gamma = 2.5$, $B = 15$ m, $L_0 = 40$ dB, $d_0 = 1$ m, and $M_c = 50\,000$.

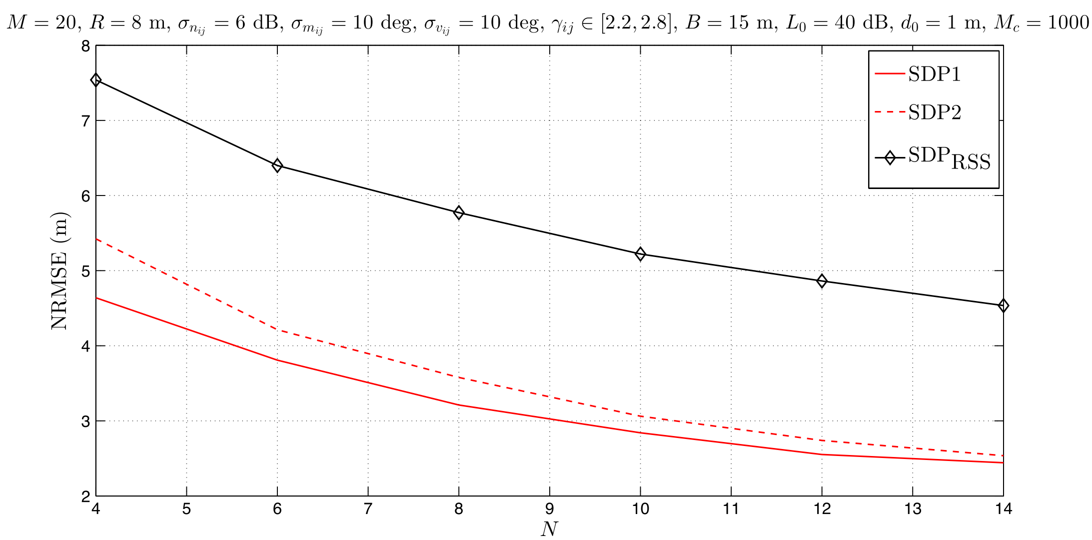

Fig. 8. NRMSE-versus-N comparison, when $M = 20$, $R = 8$ m, $\sigma_{n_{ij}} = 6$ dB, $\sigma_{m_{ij}} = 10$ deg, $\sigma_{v_{ij}} = 10$ deg, $\gamma_{ij} \in [2.2, 2.8]$, $\gamma = 2.5$, $B = 15$ m, $L_0 = 40$ dB, $d_0 = 1$ m, and $M_c = 1000$.

available in the literature. Therefore, only the performance of the proposed approaches in Section IV-A and B for both cases of known and unknown P_T values are analyzed. Here, it was assumed that the signal measurements were performed by targets. As the main performance metric, we used the normalized RMSE (NRMSE) defined as

$$\text{NRMSE} = \sqrt{\sum_{i=1}^{M_c} \sum_{j=1}^{M} \frac{\|\boldsymbol{x}_{ij} - \widehat{\boldsymbol{x}}_{ij}\|^2}{M\, M_c}}$$

where $\widehat{\boldsymbol{x}}_{ij}$ denotes the estimate of the true location of the jth target, $\boldsymbol{x}_{ij}$, in the ith M_c run.

Fig. 8 shows the NRMSE-versus-N comparison of the proposed estimators for both known and unknown P_T values and the proposed SDP method for known P_T when only RSS measurements were used, for $M = 20$, $R = 8$ m, $\sigma_{n_{ij}} = 6$ dB, $\sigma_{m_{ij}} = 10$ deg, and $\sigma_{v_{ij}} = 10$ deg. Fig. 4 confirms that adding more reliable information into the network boosts the performance of all considered estimators and decreases the performance margin between "SDP1" and "SDP2." This behavior is not unusual since by increasing N, we are expected to obtain a better estimation of P_T (*closer* to its true value) in the second step of our proposed procedure, which would enhance the estimation accuracy in the final step of the procedure. Furthermore, Fig. 8 confirms that fusing two radio measurements of the transmitted signal can significantly decrease the estimation error in comparison with using only one measurement.

Fig. 9 shows the NRMSE-versus-M comparison of the considered estimators, when $N = 8$, $R = 8$ m, $\sigma_{n_{ij}} = 6$ dB, $\sigma_{m_{ij}} = 10$ deg, and $\sigma_{v_{ij}} = 10$ deg. One can notice from Fig. 9 that adding more targets into the network does not impair the performance of the considered estimators. In fact, their performance improves as M increases. It also exhibits that the performance margin between "SDP1" and "SDP2" slowly grows with the increase of M. This might be explained by the

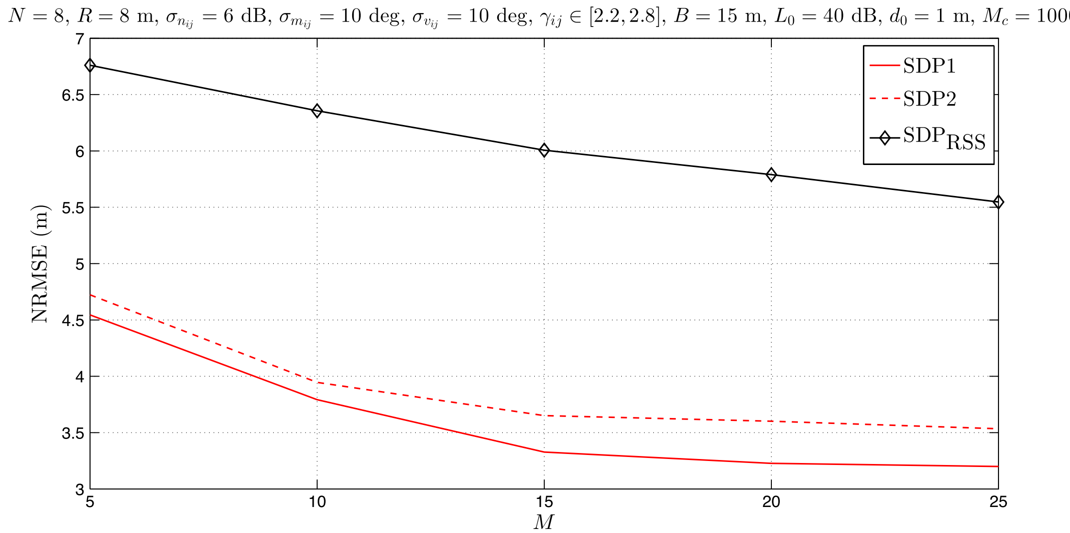

Fig. 9. NRMSE-versus-M comparison, when $N = 8$, $R = 8$ m, $\sigma_{n_{ij}} = 6$ dB, $\sigma_{m_{ij}} = 10$ deg, $\sigma_{v_{ij}} = 10$ deg, $\gamma_{ij} \in [2.2, 2.8]$, $\gamma = 2.5$, $B = 15$ m, $L_0 = 40$ dB, $d_0 = 1$ m, and $M_c = 1000$.

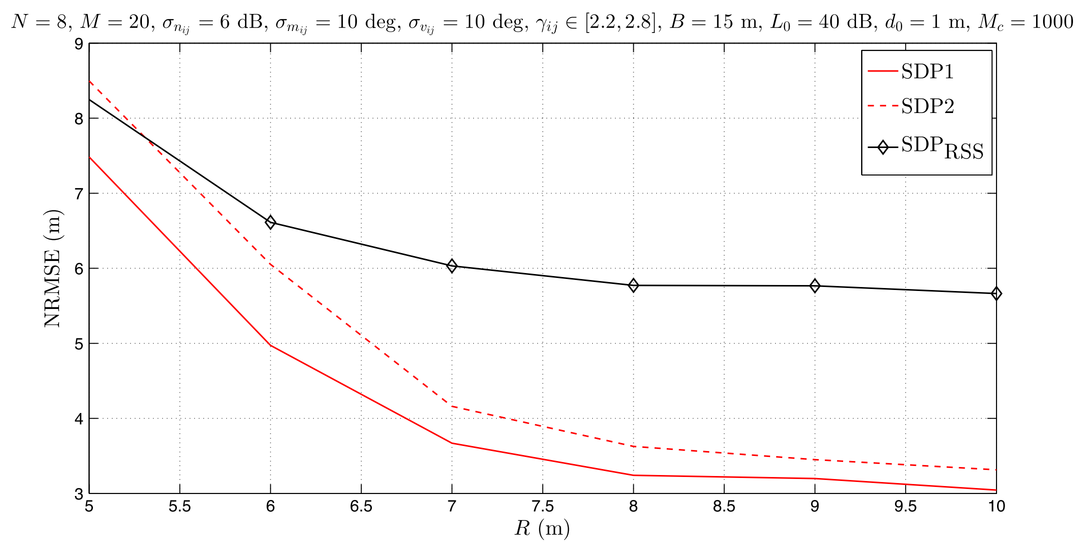

Fig. 10. NRMSE-versus-R comparison, when $N = 8$, $M = 20$, $\sigma_{n_{ij}} = 6$ dB, $\sigma_{m_{ij}} = 10$ deg, $\sigma_{v_{ij}} = 10$ deg, $\gamma_{ij} \in [2.2, 2.8]$, $\gamma = 2.5$, $B = 15$ m, $L_0 = 40$ dB, $d_0 = 1$ m, and $M_c = 1000$.

fact that when more targets are added in the network, more unreliable measurements are obtained (set $\mathcal{B}$ is enlarged), which might deteriorate the estimation of P_T and, consequently, the location estimation. Finally, although the measurement noise is high in Fig. 9, we can see that the proposed methods perform excellent.

Fig. 10 shows the NRMSE-versus-R comparison of the considered estimators, when $N = 8$, $M = 20$, $\sigma_{n_{ij}} = 6$ dB, $\sigma_{m_{ij}} = 10$ deg, and $\sigma_{v_{ij}} = 10$ deg. Fig. 10 shows that the estimation error of the new estimators decreases as R increases. This behavior is anticipated, since when R grows, the acquired information inside the network also grows, as well as the probability that more target/anchor connections are established. One can observe that the performance margin between the hybrid methods and the RSS method increases as R grows. This is because when R is too low (e.g., $R = 5$ m), the amount of information obtained from sensors is insufficient, resulting in poor estimation accuracy (NRMSE ≈ 8 m). Clearly, when R is expanded, the proposed hybrid methods benefit more from the additional links than the "SDP$_{\mathrm{RSS}}$" method, since for each additional link, two measurements (RSS and AoA) are performed. Note however that increasing R directly impacts the sensor's battery life and that, in practice, we want to keep R as low as possible.[2]

[2]The estimators in [26]–[28] and [30] were not considered here, since they were designed for 2-D scenarios, and a possible generalization to a 3-D scenario is not obvious. However, it is worth mentioning that in our simulations the proposed algorithms outperformed the mentioned algorithms in terms of the estimation accuracy in 2-D scenarios. Note also that the WLS estimator in [29] for 3-D scenarios was omitted here. The reason is that this estimator did not exhibit acceptable performance in the investigated settings, where the area accommodating nodes and the noise power are much larger than it was considered in [29].

VII. Conclusion

In this paper, we have addressed the hybrid RSS/AoA target localization problem in both noncooperative and cooperative 3-D WSNs, for both cases of known and unknown P_T values. We first developed a novel nonconvex objective function from the RSS and AoA measurement models. For the case of noncooperative localization, we showed that the derived objective function can be transformed into a GTRS framework, by following the SR approach. Moreover, we showed that the derived nonconvex objective function can be transformed into a convex objective function, by applying the SDP relaxation technique in the case of cooperative localization. For the case in which P_T is not known, we proposed a three-step procedure to enhance the estimation accuracy of our algorithms. The simulation results confirmed the effectiveness of the new algorithms in a variety of settings. For the case of noncooperative localization, the simulation results show that the proposed approaches significantly outperform the existing approach, even for the case wherein the proposed estimators have no knowledge of P_T. For the case of cooperative localization, we have investigated the influence of N, M, and R on the estimation accuracy. For all considered scenarios, the new estimators exhibited excellent performance and robustness to not knowing P_T.

Acknowledgment

The authors would like to thank the associate editor, Dr. Y. Gao, and the anonymous reviewers for their valuable comments and suggestions that greatly improved the quality of this paper.

References

[1] N. Patwari, "Location estimation in sensor networks," Ph.D. dissertation, Dept. Elect. Eng., Univ. Michigan, Ann Arbor, MI, USA, 2005.

[2] Y. Singh, S. Saha, U. Chugh, and C. Gupta, "Distributed event detection in wireless sensor networks for forest fires," in *Proc. IEEE UKSim*, Apr. 2013, pp. 634–639.

[3] Z. Rongbai and C. Guohua, "Research on major hazard installations monitoring system based on WSN," in *Proc. IEEE ICFCC*, May 2010, pp. V1-741–V1-745.

[4] Z. Dai, S. Wang, and Z. Yan, "BSHM-WSN: A wireless sensor network for bridge structure health monitoring," in *Proc. IEEE ICMIC*, Jun. 2012, pp. 708–712.

[5] L. Blazevic, J. Y. Le Boudec, and S. Giordano, "A location-based routing method for mobile ad hoc networks," *IEEE Trans. Mobile Comput.*, vol. 4, no. 2, pp. 97–110, Mar. 2005.

[6] L. Ghelardoni, A. Ghio, and D. Anguita, "Smart underwater wireless sensor networks," in *Proc. IEEEI*, Nov. 2012, pp. 1–5.

[7] T. He *et al.*, "Energy-efficient surveillance system using wireless sensor networks," in *Proc. MobiSys*, Jun. 2004, pp. 1–14.

[8] L. Buttyán and J. P. Hubaux, *Security and Cooperation in Wireless Networks: Thwarting Malicious and Selfish Behavior in the Age of Ubiquitous Computing*. Cambridge, U.K.: Cambridge Univ. Press, 2007.

[9] N. Patwari, J. N. Ash, S. Kyperountas, A. O. Hero, III, R. L. Moses, and N. S. Correal, "Locating the nodes: Cooperative localization in wireless sensor networks," *IEEE Signal Process. Mag.*, vol. 22, no. 4, pp. 54–69, Jul. 2005.

[10] G. Destino, "Positioning in wireless networks: Noncooperative and cooperative algorithms," Ph.D. dissertation, Dept. Commun. Eng., Univ. Oulu, Oulu, Finland, 2012.

[11] S. Tomic, M. Beko, and R. Dinis, "Distributed RSS-based localization in wireless sensor networks based on second-order cone programming," *Sensors*, vol. 14, no. 10, pp. 18 410–18 432, Oct. 2014.

[12] S. Tomic, M. Beko, and R. Dinis, "Distributed RSS-AoA based localization with unknown transmit powers," *IEEE Wireless Commun. Lett.*, vol. 5, no. 4, pp. 392–395, Aug. 2016.

[13] G. Wang, H. Chen, Y. Li, and N. Ansari, "NLOS error mitigation for TOA-based localization via convex relaxation," *IEEE Trans. Wireless Commun.*, vol. 13, no. 8, pp. 4119–4131, Aug. 2014.

[14] R. Kim, T. Ha, H. Lim, and D. Jung, "TDoA localization for wireless networks with imperfect clock synchronization," in *Proc. ICOIN*, Feb. 2014, pp. 417–421.

[15] J. Prieto, S. Mazuelas, A. Bahillo, P. Fernandez, R. M. Lorenzo, and E. J. Abril, "On the minimization of different sources of error for an RTT-based indoor localization system without any calibration stage," in *Proc. IEEE IPIN*, Sep. 2010, pp.1–6.

[16] Y. Wang and K. C. Ho, "An asymptotically efficient estimator in closed-form for 3D AOA localization using a sensor network," *IEEE Trans. Wireless Commun.*, vol. 14, no. 12, pp. 6524–6535, Jul. 2015.

[17] R. W. Ouyang, A. K.-S. Wong, and C.-T. Lea, "Received signal strength-based wireless localization via semidefinite programming: Noncooperative and cooperative schemes," *IEEE Trans. Veh. Technol.*, vol. 59, no. 3, pp. 1307–1318, Mar. 2010.

[18] G. Wang and K. Yang, "A new approach to sensor node localization using RSS measurements in wireless sensor networks," *IEEE Trans. Wireless Commun.*, vol. 10, no. 5, pp. 1389–1395, May 2011.

[19] G. Wang, H. Chen, Y. Li, and M. Jin, "On received-signal-strength based localization with unknown transmit power and path loss exponent," *IEEE Wireless Commun. Lett.*, vol. 1, no. 5, pp. 536–539, Oct. 2012.

[20] R. M. Vaghefi, M. R. Gholami, R. M. Buehrer, and E. G. Ström, "Cooperative received signal strength-based sensor localization with unknown transmit powers," *IEEE Trans. Signal Process.*, vol. 61, no. 6, pp. 1389–1403, Mar. 2013.

[21] S. Tomic, M. Beko, and R. Dinis, "RSS-based localization in wireless sensor networks using convex relaxation: Noncooperative and cooperative schemes," *IEEE Trans. Veh. Technol.*, vol. 64, no. 5, pp. 2037–2050, May 2015.

[22] A. Bahillo *et al.*, "Hybrid RSS-RTT localization scheme for indoor wireless networks," *EURASIP J. Advance Sig. Process.*, vol. 2010, no. 1, pp. 1–12, Mar. 2010.

[23] U. Hatthasin, S. Thainimit, K. Vibhatavanij, N. Premasathian, and D. Worasawate, "The use of RTOF and RSS for a one base station RFID system," *Int. J. Comput. Sci. Netw. Security*, vol. 10, no. 7, pp. 862–865, Jul. 2010.

[24] T. Gädeke, J. Schmid, M. Krüger, J. Jany, W. Stork, and K. D. Müller-Glaser, "A bi-modal ad-hoc localization scheme for wireless networks based on RSS and ToF fusion," in *Proc. IEEE WPNC*, Mar. 2013, pp. 1–6.

[25] K. Yu, "3-D localization error analysis in wireless networks," *IEEE Trans. Wireless Commun.*, vol. 6, no. 10, pp. 3473–3481, Oct. 2007.

[26] S. Wang, B. R. Jackson, and R. Inkol, "Hybrid RSS/AOA emitter location estimation based on least squares and maximum likelihood criteria," in *Proc. IEEE QBSC*, Jun. 2012, pp. 24–29.

[27] L. Gazzah, L. Najjar, and H. Besbes, "Selective hybrid RSS/AOA approximate maximum likelihood mobile intra cell localization," in *Proc. EW*, Apr. 2013, pp. 1–6.

[28] L. Gazzah, L. Najjar, and H. Besbes, "Selective hybrid RSS/AOA weighting algorithm for NLOS intra cell localization," in *Proc. IEEE WCNC*, Apr. 2014, pp. 2546–2551.

[29] Y. T. Chan, F. Chan, W. Read, B. R. Jackson, and B. H. Lee, "Hybrid localization of an emitter by combining angle-of-arrival and received signal strength measurements," in *Proc. IEEE CCECE*, May 2014, pp. 1–5.

[30] P. Biswas, H. Aghajan, and Y. Ye, "Semidefinite programming algorithms for sensor network localization using angle of arrival information," in *Proc. Asilomar Conf. Signals, Syst., Comput.*, Oct. 2005, pp. 220–224.

[31] P. Biswas, T.-C. Lian, T.-C. Wang, and Y. Ye, "Semidefinite programming based algorithms for sensor network localization," *ACM Trans. Sens. Netw.*, vol. 2, no. 2, pp. 188–220, May 2006.

[32] R. Fletcher, *Practical Methods of Optimization*. Chichester, U.K.: Wiley, 1987.

[33] A. Beck, P. Stoica, and J. Li, "Exact and approximate solutions of source localization problems," *IEEE Trans. Signal Process.*, vol. 56, no. 5, pp. 1770–1778, May 2008.

[34] Z. Xiang and U. Ozguner, "A 3-D positioning system for off-road autonomous vehicles," in *Proc. IEEE IV*, Jun. 2005, pp. 130–134.

[35] T. S. Rappaport, *Wireless Communications: Principles and Practice*. Upper Saddle River, NJ, USA: Prentice-Hall, 1996.

[36] M. L. Sichitiu and V. Ramadurai, "Localization of wireless sensor networks with a mobile beacon," in *Proc. IEEE MASS*, Oct. 2004, pp. 174–183.

[37] S. M. Kay, *Fundamentals of Statistical Signal Processing: Estimation Theory*. Upper Saddle River, NJ, USA: Prentice-Hall, 1993.

[38] I. J. Myung, “Tutorial on maximum likelihood estimation,” *J. Math. Psychol.*, vol. 47, no. 1, pp. 90–100, Feb. 2003.

[39] S. Boyd and L. Vanderberghe, *Convex Optimization*. Cambridge, U.K.: Cambridge Univ. Press, 2004.

[40] J. J. More, “Generalization of the Trust Region Problem,” *Optim. Meth. Softw.*, vol. 2, pp. 189–209, 1993.

[41] M. Grant and S. Boyd, *CVX: Matlab Software for Disciplined Convex Programming*, (accessed on Apr. 15, 2010), Version 1.21. [Online]. Available: http://cvxr.com/cvx

[42] I. Pólik and T. Terlaky, “Interior point methods for nonlinear optimization,” in *Nonlinear Optimization*, 1st ed., G. Di Pillo and F. Schoen, Eds. New York, NY, USA: Springer-Verlag, 2010.

[43] J. F. Sturm, “Using SeDuMi 1.02, a MATLAB Toolbox for Optimization Over Symmetric Cones,” *Optim. Meth. Softw.*, vol. 11, no. 12, pp. 625–653, 1998.

Slavisa Tomic received the M.S. degree in traffic engineering, under the Postal Traffic and Telecommunications Study program, from the University of Novi Sad, Novi Sad, Serbia, in 2010. He is currently working toward the Ph.D. degree with the Department of Electrical and Computer Engineering, Universidade Nova de Lisboa, Lisbon, Portugal.

His research interests include target localization in wireless sensor networks and convex optimization.

Marko Beko was born in Belgrade, Serbia, on November 11, 1977. He received the Dipl.-Ing. degree from the University of Belgrade, Belgrade, in 2001 and the Ph.D. degree in electrical and computer engineering from Instituto Superior Técnico, Lisbon, Portugal, in 2008.

He is currently an Associate Professor with the Universidade Lusófona de Humanidades e Tecnologias, Lisbon. He is also a Researcher with the Centre of Technology and Systems, Instituto de Desenvolvimento de Novas Tecnologias (UNINOVA), Faculdade de Ciências e Tecnologia, Universidade Nova de Lisboa, Caparica, Portugal. His research interests include signal processing for wireless communications and nonsmooth and convex optimization.

Dr. Beko is an Associate Editor of the *Radioengineering Journal*. He received the 2008 IBM Portugal Scientific Award.

Rui Dinis (M’00–SM’14) received the Ph.D. degree from Instituto Superior Técnico (IST), Technical University of Lisbon, Lisbon, Portugal, in 2001 and the Habilitation degree in telecommunications from Faculdade de Ciências e Tecnologia (FCT), Universidade Nova de Lisboa (UNL), Caparica, Portugal, in 2010.

From 2001 to 2008, he was a Professor with IST. He is currently an Associate Professor with FCT-UNL. In 2003, he was an Invited Professor with Carleton University, Ottawa, ON, Canada. He was a Researcher with Centro de Análise e Processamento de Sinal, IST, from 1992 to 2005 and with Instituto de Sistemas e Robótica from 2005 to 2008. Since 2009, he has been a Researcher with Instituto de Telecomunicações, Lisboa, Portugal.

Dr. Dinis has been an Editor of the IEEE TRANSACTIONS ON COMMUNICATIONS (Transmission Systems—Frequency-Domain Processing and Equalization) since 2012 and of the IEEE TRANSACTIONS ON VEHICULAR TECHNOLOGY since 2015. He was also a Guest Editor of Elsevier’s *Physical Communication* (Special Issue on Broadband Single-Carrier Transmission Techniques). He was a Technical Program Committee Chair of the 2014 IEEE International Conference on Telecommunications. He has been actively involved in several international research projects in the broadband wireless communications area.